Surface spin waves in a semi-infinite ferromagnet with perpendicular surface anisotropy

1994 J. Phys.: Condens. Matter 6 9613

(http://iopscience.iop.org/0953-8984/6/45/011)

J. Phys.: Condens. Matter 6 (1994) 9613–9620. Printed in the UK

Surface spin waves in a semi-infinite ferromagnet with perpendicular surface anisotropy

Yoshikazu Endo

Physics Laboratory, The Nippon Dental University, Fujimi, Chiyoda-ku, Tokyo 102, Japan

Received 21 July 1994

Abstract. The effect of perpendicular surface anisotropy on surface spin-wave excitations in a semi-infinite ferromagnet is studied by solving the coupled equations of motion of spin-wave annihilation and creation operators. The ground-state spin arrangement in our model is either as in-plane ordering or a canted one due to a competition between the perpendicular anisotropy in the surface and the bulk anisotropy parallel to the surface, and surface spin-wave frequencies are calculated in both phases. It is shown that at the transition point between these two distinct phases a low-lying surface spin-wave branch becomes soft, and consequently the ellipticity and the amplitude of spin precessions in the surface layer grow large in the vicinity of the transition point.

1. Introduction

In recent experiments large perpendicular anisotropy has been found at the surfaces of magnetic thin films and semi-infinite magnets, and spin reorientation phenomena caused by a change in the film thickness or temperature have been extensively studied [1–4]. The preferred direction of magnetization in such materials is, in general, parallel to the surface because of a shape anisotropy. Surfaces, however, can possess a perpendicular anisotropy in consequence of the reduced symmetry, so that there occurs a competition between the perpendicular surface anisotropy and in-plane bulk one [5, 6]. Theoretical investigations taking into account such a competition have been performed recently for magnetic films [7, 8] and semi-infinite magnets [9–11]. The general trend is that in zero external field the direction of magnetization in thin films is either parallel or perpendicular to the surface, depending sensitively on the film thickness and temperature; for example, at low temperatures a film consisting of a few layers may have all spins normal to the surface, but for thicker films or at higher temperatures they lie parallel to the surface. On the other hand, in semi-infinite magnets spin canting may occur near the surface if the strength of the perpendicular surface anisotropy exceeds a certain critical value.

In the surface region of a semi-infinite magnet there exist surface spin waves reflecting the spin arrangement at and near the surface [12, 13]. Surface spin waves in an exchange-coupled semi-infinite ferromagnet have been studied by De Wames and Walfram [14], and recently their study has been extended by Gopalan and Cottam [15] to the system with single-ion uniaxial and non-uniaxial anisotropy, and Shen and Li [16] to a ferrimagnet. The studies of these authors have been concerned with the case where the surface and the bulk have the same easy direction of magnetization. If the surface anisotropy is non-collinear with the bulk one, as encountered in the system with dominant perpendicular surface anisotropy,

0953-8984/94/459613+08$19.50

spin canting will appear near the surface. The surface spin waves may then be described by the precession of spins around the equilibrium direction specified by a layer-dependent canting angle.

The purpose of this paper is to investigate the effect of perpendicular surface anisotropy on surface spin-wave excitations in a semi-infinite Heisenberg ferromagnet. In an exchange-coupled system a simple expression for the anisotropy on the surface may be either a single-ion uniaxial anisotropy of the form $-D(S^z)^2$ or Ising-like one. In this paper we assume the latter in the perpendicular direction to the surface. In the bulk, though long-ranged dipolar interactions play an important role in determining the easy direction of the bulk spins, we assume for simplicity an Ising-like exchange anisotropy also in the planes parallel to the surface. In section 2 we propose a model Hamiltonian, and write the equations of motion for spin-wave operators. In section 3 the method used for obtaining surface spin-wave frequencies is given. In section 4 we present the results for numerical calculations together with features of the precession of spins in the surface layer.

2. Model Hamiltonian and equation of motion

We consider a spin-S semi-infinite ferromagnet with a simple-cubic structure. The xy plane is taken to lie in the surface layer and the z axis is taken normal to the surface. The bulk spins are assumed to lie in the xy plane, while the surface spins orient preferentially to the z direction. To describe such a system, we set up a model Hamiltonian

$$H = -J \sum_{(lj,l'j')} (\eta_{ll'} S^z_{lj} S^z_{l'j'} + \zeta_{ll'} S^x_{lj} S^x_{l'j'} + S^y_{lj} S^y_{l'j'}) \tag{1}$$

where J represents the ferromagnetic exchange interaction between nearest-neighbour spins, and l denotes the layer index; $l = 1$ the surface layer, $l = 2, 3, \cdots$ the inner layers, and j denotes lattice points in the xy plane. We put η_{11} ($\equiv \eta_s$) > 1 and ζ_{ll} ($\equiv \zeta_b$) > 1 for $l = 2, 3, \cdots$, and otherwise $\eta_{ll'} = \zeta_{ll'} = 1$, i.e. the spins in the surface layer have the Ising-like anisotropy in the z direction, whereas those in the inner layers have the Ising-like one in the x direction.

At low temperatures the spins described by the Hamiltonian (1) may be in general in a canted state, where the spins in the surface region cant with a layer-dependent canting angle. To characterize the spin canting, we choose a layer-dependent coordinate system x'_l, y'_l, z'_l by rotating by angle θ_l about y axis as shown in figure 1, and rewrite the Hamiltonian (1) by the new coordinate system. Then introducing annihilation and creation operators a_{lj} and $a^\dagger_{lj}$ by use of the Holstein–Primakoff transform, and making use of the linear spin-wave approximation, we have a constant term, and first- and second-order terms in the boson representation of the Hamiltonian. The direction of each z'_l axis is chosen by vanishing the first order terms, which leads to

$$\theta_l = \tan^{-1} \frac{E_l}{K_l} \tag{2}$$

with

$$E_l = 4\eta_{ll}\mu_l + \mu_{l-1} + \mu_{l+1} \qquad K_l = 4\zeta_{ll}\tau_l + \tau_{l-1} + \tau_{l+1} \tag{3}$$

where

$$\mu_l = \sin\theta_l \qquad \tau_l = \cos\theta_l. \tag{4}$$

Here and hereafter the variables with layer index 0 should vanish due to the boundary condition at the surface.

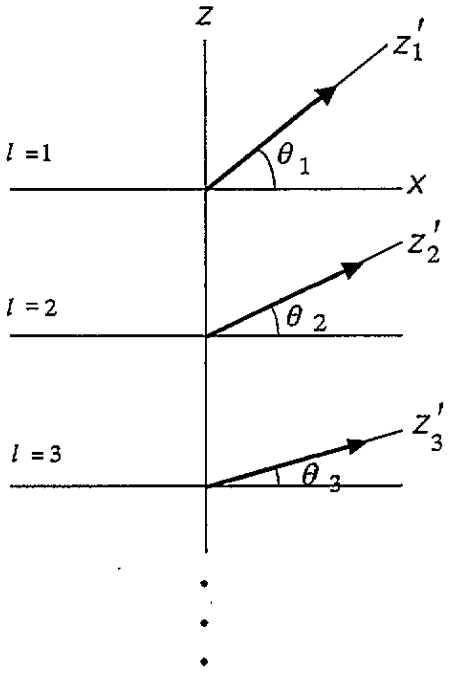

Figure 1. Schematic view of the coordinate system and the spin canting angle θ_l.

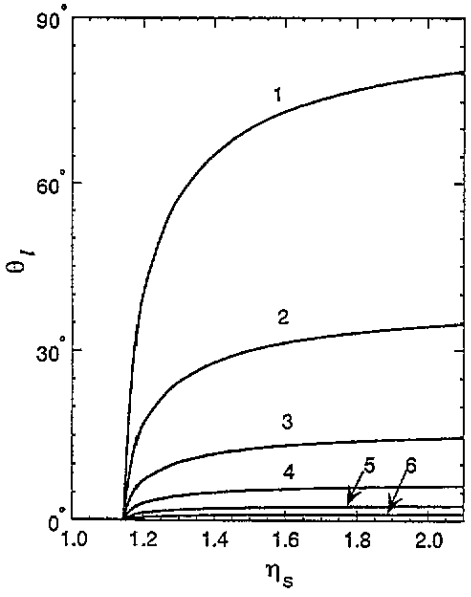

Figure 2. Spin canting angle θ_l as a function of the surface anisotropy η_s. The number attached to each curve represents the layer index.

The second-order terms of the Hamiltonian may be written, in units with $JS = 1$, as

$$H_2 = \sum_{k_\parallel,l,\rho} [A_l a^\dagger_{k_\parallel l} a_{k_\parallel l} - B_{l,l+\rho}(a^\dagger_{k_\parallel,l+\rho} a_{k_\parallel l} + a^\dagger_{k_\parallel l} a_{k_\parallel,l+\rho}) + C_l(a^\dagger_{k_\parallel l} a^\dagger_{-k_\parallel l} + a_{k_\parallel l} a_{-k_\parallel l}) - D_{l,l+\rho}(a^\dagger_{k_\parallel l} a^\dagger_{-k_\parallel,l+\rho} + a_{k_\parallel l} a_{-k_\parallel,l+\rho})] \tag{5}$$

where $a_{k_\parallel l}$ and $a^\dagger_{k_\parallel l}$ are respectively the two-dimensional Fourier transform of a_{lj} and $a^\dagger_{lj}$, $k_\parallel = (k_x, k_y)$, $\rho = \pm 1$ and

$$\begin{aligned} A_l &= \frac{1}{2}(E_l\mu_l + K_l\tau_l) - (\eta_{ll}\tau_l^2 + \zeta_{ll}\mu_l^2 + 1)\gamma_{k_\parallel} \\ B_{l,l+\rho} &= \frac{1}{4}(\tau_l\tau_{l+\rho} + \mu_l\mu_{l+\rho} + 1) \\ C_l &= -\frac{1}{2}(\eta_{ll}\tau_l^2 + \zeta_{ll}\mu_l^2 - 1)\gamma_{k_\parallel} \\ D_{l,l+\rho} &= \frac{1}{4}(\tau_l\tau_{l+\rho} + \mu_l\mu_{l+\rho} - 1) \end{aligned} \tag{6}$$

with $\gamma_{k_\parallel} = \frac{1}{2}(\cos k_x + \cos k_y)$.

The equation of motion for $a_{k_\parallel l}$ couples with that for $a^\dagger_{k_\parallel l}$, and after introducing the frequency Fourier transform, we have these equations of motion (in units of $\hbar$) in a matrix form

$$\begin{bmatrix} \omega\mathbf{I}-\mathbf{A} & -\mathbf{C} \\ \mathbf{C} & \omega\mathbf{I}+\mathbf{A} \end{bmatrix}\begin{bmatrix} a \\ a^{\dagger} \end{bmatrix}=0 \tag{7}$$

where $\mathbf{I}$ denotes a unit matrix,

$$\mathbf{A}=\begin{bmatrix} a_1 & -b_1 & & & \\ -b_1 & a_2 & -b_2 & & \\ & -b_2 & a_3 & -b_3 & \\ & & \ddots & \ddots & \ddots \end{bmatrix} \qquad \mathbf{C}=\begin{bmatrix} c_1 & -d_1 & & & \\ -d_1 & c_2 & -d_2 & & \\ & -d_2 & c_3 & -d_3 & \\ & & \ddots & \ddots & \ddots \end{bmatrix} \tag{8}$$

with $a_l = 2A_l$, $b_l = 2B_{l,l+1} = 2B_{l+1,l}$, $c_l = 4C_l$, $d_l = 2D_{l,l+1} = 2D_{l+1,l}$, and

$$a=\begin{bmatrix} a_{k_{\parallel}1}(\omega) \\ a_{k_{\parallel}2}(\omega) \\ \vdots \end{bmatrix} \qquad a^{\dagger}=\begin{bmatrix} a^{\dagger}_{-k_{\parallel}1}(\omega) \\ a^{\dagger}_{-k_{\parallel}2}(\omega) \\ \vdots \end{bmatrix}. \tag{9}$$

3. Surface spin waves

Spin-wave spectra including the surface spin waves can be obtained by vanishing the determinant of the coefficient matrix in equation (7), which is equivalent to solving

$$\det(\mathbf{H}^{+}\mathbf{H}^{-}-\omega^2\mathbf{I})=0 \qquad \text{or} \qquad \det(\mathbf{H}^{-}\mathbf{H}^{+}-\omega^2\mathbf{I})=0 \tag{10}$$

where $\mathbf{H}^{\pm} = \mathbf{A} \pm \mathbf{C}$. In the bulk $\tau_l = 1$, $\mu_l = 0$, $\eta_{ll} = 1$, $\zeta_{ll} = \zeta_b$, then $a_l = 2[2(\zeta_b - \gamma_{k_{\parallel}}) + 1] \equiv a_b$, $b_l = 1$, $c_l = d_l = 0$ in equation (8). Defining

$$\mathbf{H}_0=\begin{bmatrix} a_b & -1 & & & \\ -1 & a_b & -1 & & \\ & -1 & a_b & -1 & \\ & & \ddots & \ddots & \ddots \end{bmatrix} \tag{11}$$

and

$$\mathbf{V}=\mathbf{H}^{+}\mathbf{H}^{-}-\mathbf{H}_0^2 \qquad \mathbf{G}^{\pm}=(\mathbf{H}_0 \pm \omega\mathbf{I})^{-1} \qquad \mathbf{G}=\mathbf{G}^{+}\mathbf{G}^{-}=\mathbf{G}^{-}\mathbf{G}^{+} \tag{12}$$

we can change equation (10) into a more convenient form

$$\det(\mathbf{I}+\mathbf{G}\mathbf{V})=0 \tag{13}$$

to calculate surface spin-wave spectra. The elements of $\mathbf{G}^{\pm}$ are known as [14, 17]

$$G^{\pm}_{mn}=\frac{(x^{\pm})^{m+n}-(x^{\pm})^{|m-n|}}{x^{\pm}-(x^{\pm})^{-1}} \tag{14}$$

and so

$$G_{mn}=\frac{x^{+}x^{-}}{(1-x^{+}x^{-})(x^{+}-x^{-})}(G^{+}_{mn}-G^{-}_{mn}) \tag{15}$$

with

$$x^{\pm}+\frac{1}{x^{\pm}}=a_b \pm \omega. \tag{16}$$

The elements of **V** are calculated from the first equation of (12): for the diagonal elements

$$\begin{aligned} V_{11} &= a_1^+ a_1^- + b_1^+ - a_b^2 - 1 \\ V_{ll} &= a_l^+ a_l^- + b_{l-1}^+ + b_l^+ - a_b^2 - 2 \qquad (l \geqslant 2) \end{aligned} \tag{17}$$

and for the off-diagonal elements

$$\begin{aligned} V_{l,l+1} &= -a_l^+ - b_l^+ a_{l+1}^- + 2a_b \\ V_{l+1,l} &= -a_{l+1}^+ - b_l^+ a_l^- + 2a_b \\ V_{l,l+2} &= b_l^+ - 1 \\ V_{l+2,l} &= b_{l+1}^+ - 1 \qquad (l \geqslant 1) \end{aligned} \tag{18}$$

where $a_l^\pm = a_l \pm c_l$, $b_l^+ = b_l + d_l$.

4. Numerical results and discussion

In this section we illustrate the results for the spin canting angle and surface spin-wave dispersion in the case $\zeta_b = 1.2$. In figure 2 the spin canting angle θ_l in each layer measured with respect to the plane parallel to the surface is shown as a function of η_s. In obtaining θ_l, we have solved self-consistently the equations (2), (3) and (4) by using a simple iteration procedure for a symmetric film with thickness 100, which is enough to reproduce the bulk state. As follows from figure 2, for η_s less than 1.145 all the spins align in plane, while when η_s exceeds the critical value the spins in the surface cant abruptly out of the surface plane. The fact that the spin canting occurs abruptly at the transition point with the infinite slope such as shown in the θ_1 curve versus η_s has been pointed out by O'Handley and Woods [10] using a classical continuum model. The critical value $\eta_s^c = 1.145$ can be obtained analytically from the condition that the in-plane ordering state having $\tau_l = 1$ and $\mu_l = 0$ becomes soft at $\eta_s = \eta_s^c$, i.e. if we set $\omega = 0$ when $k_\parallel = 0$ in equation (10), then $\det \mathbf{H}^+ = 0$ leads to

$$\eta_s^c = \tfrac{1}{2}[3 - \zeta_b + \sqrt{\zeta_b(\zeta_b - 1)}]. \tag{19}$$

The penetration depth of the canted region depends mainly on the magnitude of ζ_b. As $\zeta_b \to 1$, the canted region extends deeper into the interior. On the other hand, if ζ_b is large enough, only the spins in the surface layer cant significantly, whereas those of inner layers lie in plane.

Once the ground-state spin configuration is determined, surface spin-wave spectra can be calculated from equation (13). Since $\tau_l = 1$ and $\mu_l = 0$ in the in-plane ordering state, equation (13) reduces to a 2×2 determinant. In the canted state, however, the perturbation matrix **V** does not localize in a small size, and therefore we assume that the canted region penetrates into interior up to Nth layer from the surface and the layers more than Nth are the bulk. Then the perturbation matrix **V** becomes $N+2$ by $N+2$ matrix. In order to find the surface modes lying above or below the bulk continuum using a common procedure for both the in-plane ordering and the canted states, we search numerically the solutions of equation (13) by choosing x^- as an independent variable. The domain of x^- is

$$1 \geqslant x^- \geqslant \tfrac{1}{2}(a_b - \sqrt{a_b^2 - 4}) \qquad 0 > x^- \geqslant -1 \tag{20}$$

respectively for below and above the bulk continuum. From equation (16) x^+ is dependent on x^- such that $x^+ = \frac{1}{2}[e - (e^2 - 4)^{1/2}]$ with $e = 2a_b - (x^- + 1/x^-)$.

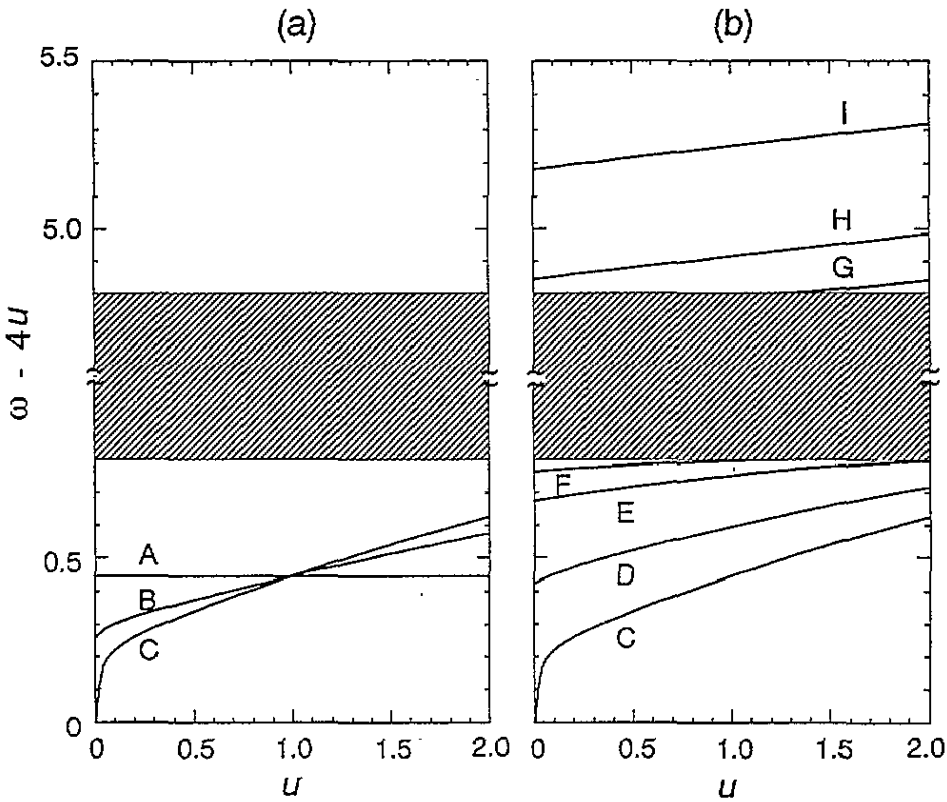

Figure 3. Surface spin-wave frequency versus $u = 1 - \gamma_{k_\parallel}$ in (a) in-plane ordering state and (b) canted state: $\eta_s = 1.0$ (A), 1.1 (B), 1.145 (C), 1.2 (D), 1.3 (E), 1.4 (F), 1.95 (G), 2.0 (H), 2.1 (I). Hatched area represents the bulk continuum.

In figure 3 the η_s dependence of the surface spin-wave dispersion in the case $\zeta_b = 1.2$ is illustrated for (a) in-plane ordering state and (b) canted state as a function of $u = 1 - \gamma_{k_\parallel}$. We have chosen $N = 8$ which is sufficient to reach the bulk magnetization as follows from figure 2. Since the ordinate measures $\omega - 4u$, the bulk continuum $\omega_{\text{bulk}} = a_b - 2\cos k_z$ represented by hatched area lies between the horizontal lines $\omega - 4u = 4(\zeta_b - 1)$ and $4\zeta_b$. In the in-plane ordering state a single surface spin-wave branch exists below the bulk continuum. As η_s increases, the gap of the surface mode with $k_\parallel = 0$ ($u = 0$) decreases, and at $\eta_s = \eta_s^c = 1.145$ the surface mode becomes soft, where a surface phase transition occurs. For η_s beyond η_s^c, the spins at and near the surface cant in the xz plane. The surface spin-wave branch shifts upward with increasing η_s and then merges into the bulk continuum. For η_s larger than about 1.93 a surface spin-wave branch appears above the bulk continuum.

It is of interest to examine the nature of the precession of spins at and near the surface. For this purpose we have to find the eigenvector corresponding to each surface spin-wave branch. Since the surface perturbation does not localize in a small size and in addition spin precessions may not be circular but elliptic, it would be difficult to find a simple expression. Instead of treating the full matrix, we confine our attention to the spins in the surface layer and fix the spins in the inner layers in the in-plane direction. Then we need only consider the terms with layer index I in equation (5), and the canting angle θ_1, spin-wave frequency

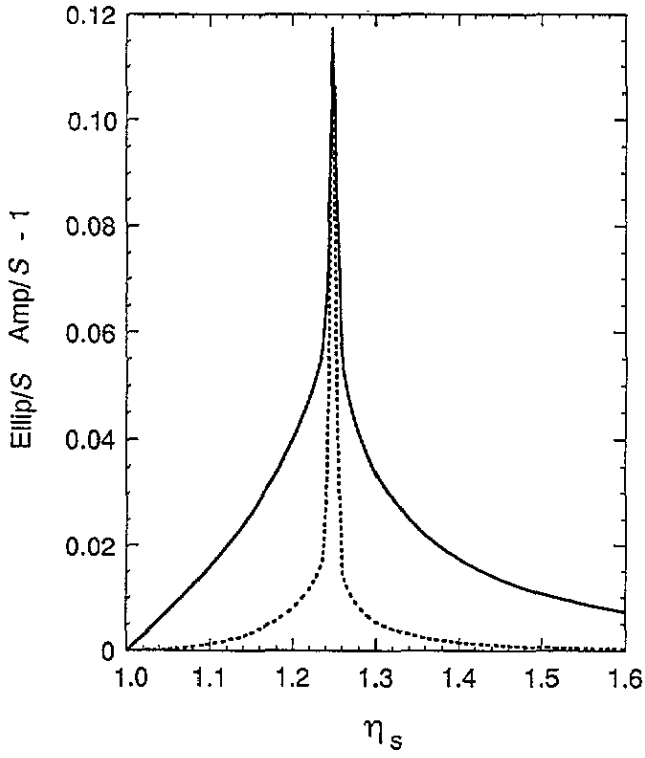

Figure 4. Ellipticity Ellip/S(solid line) and the mean-squared amplitude Amp/$S-1$(dotted line) of the spin precession in the surface layer as a function of the surface anisotropy η_s at $k_BT/SJ = 0.1$.

ω_1 and eigenvector $b_{k_\parallel 1}$ can easily be obtained as

$$\theta_1 = \tan^{-1}\frac{E_1}{K_1} \qquad \omega_1 = \sqrt{a_1^2 - c_1^2} \qquad b_{k_\parallel 1} = \cosh\phi_{k_\parallel} a_{k_\parallel 1} - \sinh\phi_{k_\parallel} a^\dagger_{-k_\parallel 1} \tag{21}$$

with $\tanh 2\phi_{k_\parallel} = -c_1/a_1$. With the aid of these expressions we can calculate the ellipticity Ellip and mean squared amplitude Amp of the spin precession [15]

$$\begin{aligned} \text{Ellip} &= \langle (S^{x'}_{1j})^2 - (S^{y'}_{1j})^2 \rangle = -\frac{S}{N_\parallel}\sum_{k_\parallel}\frac{c_1}{\omega_1}\coth\left(\frac{\beta\omega_1}{2}\right) \\ \text{Amp} &= \langle (S^{x'}_{1j})^2 + (S^{y'}_{1j})^2 \rangle = \frac{S}{N_\parallel}\sum_{k_\parallel}\frac{a_1}{\omega_1}\coth\left(\frac{\beta\omega_1}{2}\right) \end{aligned} \tag{22}$$

where $N_\parallel$ is the number of atoms in the surface layer and $\beta = SJ/k_BT$. The spin deviation $\Delta S = S - \langle S^{z'}_{1j}\rangle$ is related to Amp via $\Delta S = \frac{1}{2}(\text{Amp}/S - 1)$. The canting angle θ_1 and the frequency ω_1 show respectively similar tendencies to the curves shown in figures 2 and 3 except that $\eta_s^c = 1.25$. In figure 4 Ellip/S and Amp/$S-1$ are plotted at $k_BT/SJ = 0.1$. It follows that as η_s approaches the critical anisotropy η_s^c from either above or below, Ellip/S, Amp/$S-1$, and hence ΔS grow large, and right at $\eta_s = \eta_s^c$ they diverge. Erickson and Mills [8] have shown in their study of reorientation of spins in thin films induced by an external

field that only ultrathin films exhibit a divergence in the spin deviation at the transition point and it is less pronounced as the film thickness increases. Similarly, if we could include the inner layers in our calculation in this paragraph, the divergence of Ellip and Amp at the transition point would be depressed.

In this paper we have used a simple exchange-coupled model to take into account an interplay of the perpendicular anisotropy at the surface and the in-plane bulk one near the surface. We believe that our model describes the characteristic features of the surface spin-wave excitations in systems with non-collinear anisotropy.

References

[1] Purcell S T, Heinrich B and Arrott A S 1991 *J. Appl. Phys.* **64** 5337
[2] Pappas P, Kämper K-P and Hopster H 1990 *Phys. Rev. Lett.* **64** 3179
[3] Allenspach R and Bischof A 1992 *Phys. Rev. Lett.* **69** 3385
[4] A recent review of surface magnetism and surface anisotropy has been given by Kaneyoshi: Kaneyoshi T 1991 *J. Phys.: Condens. Matter* **3** 4497
[5] Néel L 1954 *J. Physique Radium* **15** 225
[6] Gay J G and Richter R 1987 *J. Appl. Phys.* **61** 3362
[7] Jensen P J and Bennemann K H 1990 *Phys. Rev.* B **42** 849
[8] Erickson R P and Mills D L 1991 *Phys. Rev.* B **43** 10715; *Phys. Rev.* B **44** 11825; *Phys. Rev.* B **46** 861
[9] Mills D L 1989 *Phys. Rev.* B **39** 12306
[10] O'Handley R C and Woods J P 1990 *Phys. Rev.* B **42** 6568
[11] Endo Y 1992 *Phys. Rev.* B **46** 11129
[12] Wolfram T and De Wames R E 1972 *Prog. Surf. Sci.* **2** 233
[13] Cottam M G and Tilley D R 1989 *Introduction to Surface and Superlattice Excitations* (Cambridge: Cambridge University Press)
[14] De Wames R E and Wolfram T 1969 *Phys. Rev.* **185** 720
[15] Gopalan S and Cottam M G 1990 *Phys. Rev.* B **42** 624
[16] Shen W-Z and Li Z-Y 1993 *Phys. Rev.* B **47** 2636
[17] Cottam M G 1976 *J. Phys. C: Solid State Phys.* **9** 2121